RESEARCH ARTICLE

Dynamic regulation of *N*-acyl-homoserine lactone production and degradation in *Pseudomonas putida* IsoF

Agnes Fekete[1], Christina Kuttler[2], Michael Rothballer[3], Burkhard A. Hense[4], Doreen Fischer[3], Katharina Buddrus-Schiemann[3], Marianna Lucio[1], Johannes Müller[2], Philippe Schmitt-Kopplin[1] & Anton Hartmann[3]

[1]Institute of Ecological Chemistry, Helmholtz Zentrum München, Neuherberg, Germany; [2]Centre for Mathematical Sciences, Technical University Munich, Garching, Germany; [3]Department Microbe–Plant Interactions, Helmholtz Zentrum München, Neuherberg, Germany; and [4]Institute of Biomathematics and Biometry, Helmholtz Zentrum München, Neuherberg, Germany

Correspondence: Anton Hartmann, Department Microbe–Plant Interactions, Helmholtz Zentrum München, Ingolstädter Landstr. 1, D-85764 Neuherberg, Germany. Tel.: +49 89 3187 3481; fax: +49 89 3187 3313; e-mail: anton.hartmann@helmholtz-muenchen.de

Received 27 March 2009; revised 23 November 2009; accepted 26 November 2009.
Final version published online 21 January 2010.

DOI:10.1111/j.1574-6941.2009.00828.x

Editor: Philippe Lemanceau

Keywords
Pseudomonas putida; quorum sensing; *N*-acyl-homoserine lactones; AHL-production kinetic; lactonase; mathematical model.

Abstract

The biocontrol strain *Pseudomonas putida* IsoF, which was isolated from a tomato rhizosphere, is a known *N*-acyl-homoserine lactone (AHL) producer with only one LuxI/LuxR-like quorum-sensing (QS) system. The production and degradation of AHLs were analysed in different growth phases of the bacterium. Using the analytical tools of ultra performance liquid chromatography and high resolution MS, it was possible to determine not only the various AHLs synthesized over time but also their degradation products. 3-oxo-decanoyl-homoserine lactone was found to be the dominant AHL, which reached its maximum in the early logarithmic growth phase. Although the pH of the medium was neutral, the AHLs were degraded thereafter rapidly to the corresponding homoserines and other metabolites. The proposed lactonase gene of *P. putida* IsoF could not be identified, because it is apparently quite different from hitherto described lactonases. The analytical data were used to calculate the rates and thresholds of AHL production by mathematical modelling, allowing quantitative predictions and a further understanding of the QS-based regulations in this bacterium. This study, combining microbiological, chemical and mathematical approaches, suggests that AHL degradation is an integral part of the whole autoinducer circuit of *P. putida* IsoF.

Introduction

Gene regulation depending on the environmental concentration of self-released diffusible substances (autoinducers) is common among bacterial species living in a variety of ecosystems (Demuth & Lamont, 2006; Williams *et al.*, 2007). It is interpreted as quorum sensing (QS), i.e. a cell-to-cell communication to drive coordinated behaviour in a cell density-dependent manner (Fuqua *et al.*, 1994). However, there are alternative concepts such as diffusion sensing or the more general efficiency sensing (Redfield, 2002; Hense *et al.*, 2007). *N*-acyl-homoserine lactones (AHLs) in Gram-negative bacteria and peptides in Gram-positive bacteria represent the main autoinducer groups. Receptor molecules in the cell membrane or the cytoplasm bind to the autoinducer and regulate the expression of a set of genes. Often, genes connected to the production of the autoinducer are upregulated, reflecting a positive feedback regulation. Based on the observation of phenotypes and pathway structures, it was conjectured that such a positive feedback results in a bistability of the system, respectively, a switch-like behaviour of the phenotype (Nealson, 1977; Dockery & Keener, 2001; Smits *et al.*, 2006). In the last few years, it became apparent that integration of autoinducer signalling in a complex regulatory network, often containing multiple autoinducer systems, enables a sophisticated fine-tuning of gene regulation in response to diverse environmental conditions.

The molecular mechanisms of autoinducer signalling are well investigated for some model organisms, but a number of aspects are still poorly understood. This especially applies to the dynamics of autoinducer concentration and its

impact on function. The positive feedback in autoinducer production was concluded from the signalling pathway structure and partly confirmed by the phenotype, for example the amount of luminescence in *Vibrio fischeri* (Nealson, 1977; Fuqua *et al.*, 1994), but the level and nature of autoinducer-compounds were hardly ever quantitatively measured directly. It had been argued that the positive feedback may play a crucial role in maintaining autoinducer systems evolutionarily stable in natural ecosystems; thus, quantitative information is highly desirable (Hense *et al.*, 2007). The threshold for induction of the positive feedback has been calculated from phenotype changes; however, this indirect determination is susceptible to the effects of stochasticity and accumulation, resulting in a low reliability (Müller *et al.*, 2008). At least some of the autoinducer-producing bacteria also synthesize autoinducer-degrading enzymes (Zhang *et al.*, 2002; Uroz *et al.*, 2008). This was suggested to be linked to the ability of the cells to quickly respond to environmental changes with a kind of system reset or simply with the use of autoinducer as a nutrient, but its real purpose is still under discussion (Zhang *et al.*, 2002; Huang *et al.*, 2003; Wang & Leadbetter, 2005; Horswill *et al.*, 2007; Wang *et al.*, 2007).

Bacterial AHL synthesis pathways produce, besides their cognate AHL, lower amounts of other AHL species (Fekete *et al.*, 2007; Ortori *et al.*, 2007). The proportions of different AHLs may vary, for example due to the different specificities of degradation enzymes (Uroz *et al.*, 2008). As the AHL receptors also show some cross reactivity (Welch *et al.*, 2000; Lee *et al.*, 2006), the dynamics of all occurring AHLs should be integrated in an interpretation of the gene regulation system. Furthermore, different degradation pathways, for example via acylase and lactonase, are known and may occur within species, further complicating a quantitative analysis of the AHL kinetics. A comprehensive understanding of the function of autoinducer signalling requires quantitative information about the dynamics of all AHLs as well as their degradation.

In recent years, it has become evident that among Gram-negative plant growth-promoting bacteria, gene regulation via AHLs is a common trait. It might be involved in bacterial rhizosphere competence, as it coordinates the expression of special phenotypes, for example the formation of biofilms, siderophore production or the production of antibiotics. One well-studied example of such an AHL-producing, plant growth-promoting rhizobacterium is *Pseudomonas putida* IsoF, which has been isolated from tomato rhizosphere (Steidle *et al.*, 2001). In this strain, a LuxI/LuxR-type QS system has been characterized, which controls the production of different types of AHLs, including 3-oxo-dodecanoyl-homoserine lactone (3-oxo-C12-HSL) and 3-oxo-decanoyl-homoserine lactone (3-oxo-C10-HSL) (Steidle *et al.*, 2002). In *P. putida* IsoF, the production of AHL signal molecules is directed by the AHL synthase PpuI, whereas the regulatory protein PpuR binds to the AHL signal molecules and controls the *ppuI* expression in a positive feedback loop (Steidle *et al.*, 2002). This system is very similar to the LasI/R system of *Pseudomonas aeruginosa*, but unlike *P. aeruginosa*, only one autoinducer system has been found in *P. putida* IsoF so far. Between *ppuI* and *ppuR* an ORF with significant similarity to the *rsaL* gene of *P. aeruginosa* and *Burkholderia kururiensis* is located, which codes for a repressor protein binding to *lasI* (Rampioni *et al.*, 2006; Suarez-Moreno *et al.*, 2008). Inactivation of this gene leads to an increase of *ppuI* expression and hence AHL production in *P. putida* WCS358 and PCL1445, *P. aeruginosa* and *B. kururiensis* (Bertani & Venturi, 2004; Dubern *et al.*, 2006; Rampioni *et al.*, 2006; Suarez-Moreno *et al.*, 2008). There is an additional gene in *P. putida* IsoF belonging to the *ppu* locus downstream of *ppuR*, which is putatively regulated by QS and termed *ppuA*. Significant similarities to long-chain fatty acid coenzyme A ligases and to nonribosomal peptide synthetases were detected, but its function has not been clarified so far (Steidle *et al.*, 2002). No functional evidence for an AHL-degrading enzyme has been found as yet in *P. putida* IsoF.

Pseudomonas putida IsoF was selected as a model organism as it contains only one (known) AHL system, simplifying understanding, and due to its potential economic relevance as a biocontrol agent (Schuhegger *et al.*, 2006). In a systems biological approach, different AHLs, their corresponding homoserines and other degradation products were determined over time in growth experiments by Fourier transform ion cyclotron MS (FT-ICR-MS) and ultra performance liquid chromatography (UPLC) combined with solid-phase extraction (SPE). Based on these quantitative, time-resolved data, mathematical modelling allowed calculation of the rates and thresholds of AHL production and could also provide an explanation for the observed rapid degradation process of AHLs in the analysed system. Only with the combination of extensive chemical and mathematical analyses were we able to demonstrate a new feature of fine-tuning of autoinducer production in *P. putida* IsoF. This may lead to an ecologically relevant and most precise adaptation of autoinducer production to changing environmental conditions.

Materials and methods

Preparation of culture supernatants

Cultures of *P. putida* strains IsoF (Steidle *et al.*, 2001), F117 (an AHL-negative *ppuI* mutant of IsoF) (Steidle *et al.*, 2002) and KT2440 were grown in ABC minimal medium (Clark & Maaløe, 1967), buffered to a pH of 6.8, to avoid abiotic degradation of AHLs (Englmann *et al.*, 2007). The pH was measured after each sampling and was never found to be

above 7.2. Cells were shaken at 30 °C and 175 r.p.m. in 500-mL baffled flasks with 200 mL of medium. Alternatively, a 5-L beaker was used containing 4 L of ABC medium, which was stirred by a magnetic stirrer at about 200 r.p.m. The medium was inoculated 1 : 1000 with an overnight culture and samples were taken right after inoculation and then every hour. The $OD_{436\,nm}$ was recorded, and an aliquot of cells was fixed with paraformaldehyde for subsequent cell counting under the microscope (10 randomly selected squares of 126 μm^2 each per time point). After taking the last sample, the ratio between living and dead cells was determined using a live/dead cell staining kit (Molecular Probes, Live/Dead BacLight Bacterial Viability Kit). The percentage of living cells at the last time point was still above 90%. The 200-mL samples collected were centrifuged at 15 000 ***g*** and 4 °C for 15 min and the supernatant was filtered through Millipore nitrocellulose filters (0.22 μm, type GSWP) with a vacuum pump. Then the samples were quenched by shock frosting with liquid nitrogen and stored at −20 °C until measured. For analysing bacterial cell pellets, the bacteria were dissolved in 2 mL ultrapure water, the same volume of methanol was added and finally they were shock frosted with liquid nitrogen.

For the spiking experiments, the inoculated medium was incubated until the $OD_{436\,nm}$ reached 0.2 and then the AHL was spiked to a final concentration of 100 nM. Sampling was performed as described above immediately after spiking and then every hour for 3 h. As a control, one last sample was obtained after 16 h.

Extraction process

The supernatants were purified by SPE and analysed afterwards by UPLC and FT-ICR-MS according to a previously published method (Li *et al.*, 2006; Fekete *et al.*, 2007). Briefly, after conditioning with methanol and water, the 200-mL sample extract that was spiked with self-synthesized internal standard (*N*-nonyloyl-homoserine lactone) was introduced onto a MegaBond Elute cartridge (Varian, Darmstadt, Germany). The cartridge was then washed with a methanol/water mixture, dried under vacuum and then the solutes were eluted with a 2-propanol/hexane mixture. The eluate was dried under a nitrogen stream, resolved with water containing 10% v/v acetonitrile and filtered through a polytetrafluoroethylene filter.

The pellets obtained from the centrifugation of the 200 mL culture supernatant were dissolved in a 4 mL methanol–water (50/50% v/v) mixture and sonicated for 15 min two times in iced water. Then the suspension was centrifuged at 8000 ***g*** and room temperature for 15 min. The supernatant was filtered through a 0.22-μm cellulose nitrate filter (VWR, Ismaning, Germany) and directly used for FT-ICR-MS analysis.

Quantification of AHL and HS concentrations with UPLC

The quantification of the AHL signal substances (Li *et al.*, 2006) and serines (Englmann *et al.*, 2007) was performed on a Waters Acquity UPLC System (Waters, Darmstadt, Germany) equipped with a 2996 PDA detector. The reversed phase separation was achieved on a BEH C_{18} packing with 1.7 μm particle diameter and column dimensions of 100 × 2.1 mm (Waters). The thermostat of the column was set to 60 °C and the autosampler to 27 °C. The flow rate was 0.9 mL min^{-1} and the injection volume was 20 μL via full loop. For the separation of the AHLs, a linear solvent strength gradient was applied starting with water containing 10% v/v acetonitrile increasing to 100% acetonitrile in 1 min. The serines were determined using a separate method with the mobile phase of 10 mM ammonium formate at pH 4.25 containing 10% v/v acetonitrile for 0.2 min following solvent gradient to 100% acetonitrile within half a minute. The detection wavelength was set to 197 nm (1.2 nm width) with the scan rate of 20 Hz. The peak areas were integrated using EMPOWER 2 (Waters).

AHL identification by FT-ICR-MS

Positive FT-ICR spectra for qualitative analysis of AHLs were acquired on a Bruker Daltonics (Bremen, Germany) Apex Qe 12T system equipped with an APOLLO II source and microspray infusion of 120 μL h^{-1} with a scan number of 256. Spectra were acquired in the broadband mode and were calibrated externally on clusters of arginine. Peaks exceeding a threshold signal-to-noise ratio of 3 were exported to peak lists. The resulting text files containing > 2300 mass–intensity pairs were scanned using a software tool written in PYTHON (http://www.python.org) for the presence of peaks from a reference file with theoretically possible protonated and sodium-cationized homoserine lactone masses with an error < 1 p.p.m. Only the *m*/*z* of those AHLs were considered for which the ^{13}C isotope peak was detectable.

Mathematical modelling

The fitting of the mathematical model to the experimental data was performed using a minimization procedure (least square method) of the software tool MATLAB, version 7.5.0.338 (R2007b, The Mathworks Inc., Natick, MA).

Results

Quantitative analysis of AHL production and degradation in liquid cultures of *P. putida* IsoF

For studying the AHL production and kinetics of *P. putida* IsoF, two different set-ups were used: (1) a 5-L beaker from

which 200 mL was taken at each time point and (2) a set of 500-mL baffled flasks each containing sample volumes of 200 mL to allow the comparison of production rates under different culture conditions. The cultures were incubated for 34 h in a well-buffered medium (pH 6.8–7.2) and grew exponentially from 6 to 13 h, followed by the late exponential phase from 13 to 19 h after inoculation (Fig. 1a). Table 1 summarizes the detected putative AHLs extracted from the supernatants. The highest *m/z* was found for 3-oxo-C10-HSL (1.7×10^9), followed by 3-oxo-C12-HSL (1.7×10^8) and 3-oxo-C8-HSL (1.4×10^7) as can be seen in Fig. 2b, as well. The other possible AHLs with lower intensity differed mostly in the saturation and/or the keto- or hydroxyl substitution of the side chain and not so much in its length.

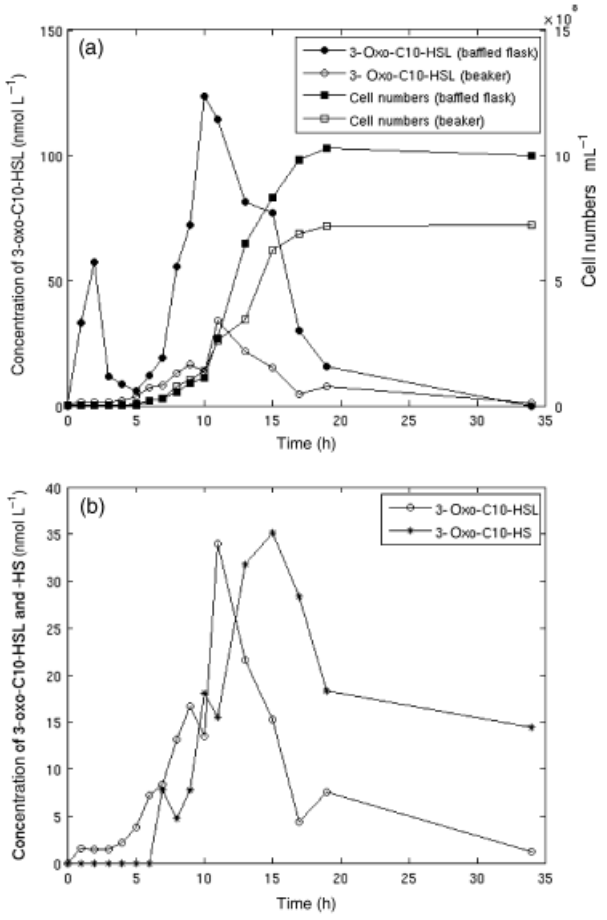

Fig. 1. Growth curve and AHL concentration. (a) The graph visualizes the growth curve of *Pseudomonas putida* IsoF and the time-resolved concentration of 3-oxo-C10-HSL produced by *P. putida* IsoF grown in a beaker (○) and baffled flasks (●) as detected by UPLC. The corresponding cell densities determined by microscopic counting are also depicted in the beaker (□) and baffled flask (■). (b) The graph shows a comparison of the time-resolved concentrations of 3-oxo-C10-HSL (○) and 3-oxo-C10-HS (∗) (as a degradation product, being further degraded itself) from the beaker experiment.

Table 1. Putative AHLs

Measured mass	Composition	Error (p.p.m.)	Putative AHL-Na	Intensity ($\times 10^6$)
250.1414	$C_{12}H_{21}NO_3Na$	0.31	C8-HSL	2.2
264.1208	$C_{12}H_{19}NO_4Na$	0.46	3-Oxo-C8-HSL	14.4
276.1571	$C_{14}H_{23}NO_3Na$	0.33	C10:1-HSL	0.9
278.1728	$C_{14}H_{25}NO_3Na$	0.55	C10-HSL	3.6
292.1521	$C_{14}H_{23}NO_4Na$	0.52	3-Oxo-C10-HSL	1679.8
294.1678	$C_{14}H_{25}NO_4Na$	0.73	3-OH-C10-HSL	5.6
304.1885	$C_{16}H_{27}NO_3Na$	0.70	C12:1-HSL	6.3
306.2042	$C_{16}H_{29}NO_3Na$	0.60	C12-HSL	8.8
318.1678	$C_{16}H_{25}NO_4Na$	0.67	3-Oxo-C12:1-HSL	7.1
320.1834	$C_{16}H_{27}NO_4Na$	0.57	3-Oxo-C12-HSL	160.8
322.1991	$C_{16}H_{29}NO_4Na$	0.66	3-OH-C12-HSL	6.2
334.2355	$C_{18}H_{33}NO_3Na$	0.82	C14-HSL	1.3
348.2150	$C_{18}H_{31}NO_4Na$	0.95	3-Oxo-C14-HSL	0.6

The various AHLs are listed as their sodium adduct with their intensity values from the extracted supernatant at 9 h measured by FT-ICR-MS. The *m/z* values provide information on elemental composition with high accuracy because the error at p.p.m. is < 1.

To confirm the identification, the same sample was separated by UPLC and detected by a photo diode array (Fekete *et al.*, 2007). Using this method, three peaks could be assigned to 3-oxo-C8-HSL, 3-oxo-C10-HSL and 3-oxo-C12-HSL (Fig. 3). The peak for 3-oxo-C10-HSL at 0.927 min showed the highest intensity. Therefore, in terms of these three components, the UPLC measurements supported the FT-ICR-MS results. Other AHLs identified by FT-ICR-MS as listed in Table 1 could not be detected with UPLC presumably due to the lower sensitivity of the method. Both methods were applied for *P. putida* F117, a mutant that is unable to produce the autoinducer (Steidle *et al.*, 2002). Because no peaks were detected at the retention time of the analytes, the sample constituents did not interfere with the targets.

Using the FT-ICR-MS method, no AHLs were able to annotate in extracts of the bacterial cell pellets. It has been determined previously that in a liquid culture medium, up to 20% of AHLs with long, nonpolar side chains can adsorb to a highly nonpolar surface (Götz *et al.*, 2007). In order to determine whether the AHLs produced by *P. putida* IsoF adsorb to the glass walls of the culture vessels or to bacterial cell walls and might therefore not be extractable, a liquid culture of the *P. putida* strain KT2440, which does not produce any AHLs and/or AHL-degrading enzymes, was spiked with 3-oxo-C10-HSL. After a 2-h incubation, 94% of the added amount could be retrieved from the culture medium supernatant; thus, no substantial physical adsorption of the AHL derivative on the cell and/or the glass surface was observed during the experiment.

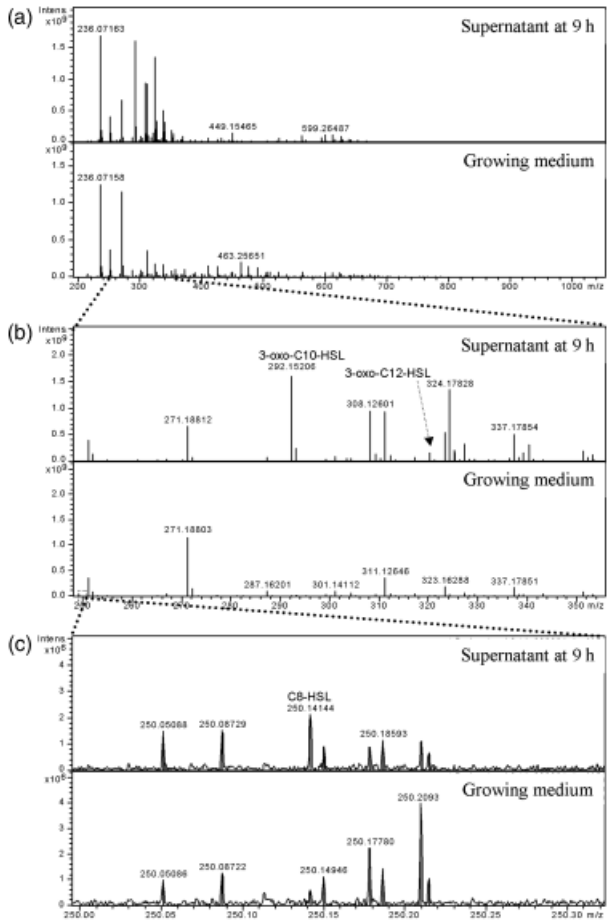

Fig. 2. FT-ICR-MS spectra of the extracted supernatant. Exponentially growing cultures in baffled flasks are shown compared with the control medium at an *m/z* range between (a) 200 and 1000, (b) 250 and 350 and (c) 250.0 and 250.3. More than 4000 peaks were detected in a broad mass range (a) due to the high resolution (> 200 000). The peaks of 3-oxo-C10-HSL and 3-oxo-C12-HSL were detectable at a high intensity in the extracted supernatant (b). Because of the high accuracy of the charged mass measurement (mass error < 0.1 p.p.m.), the elemental composition of the exact *m/z-s* can be determined (c).

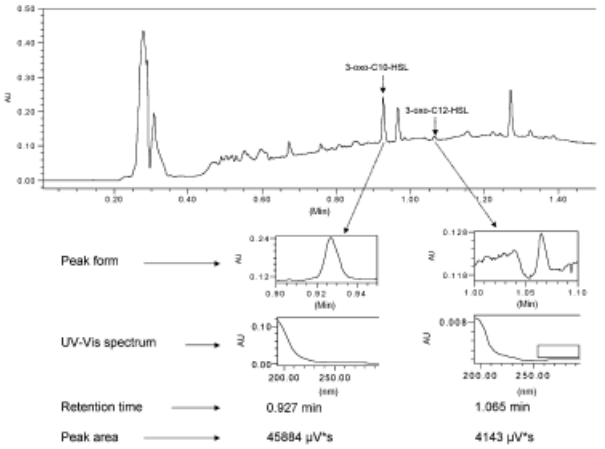

Fig. 3. Typical chromatogram of the extracted supernatant. (time point: 9 h) For the identification of the peaks, the peak form, the UV–Vis spectrum and the retention time compared with the standard were applied. The peak area was applied for quantification applying the calibration curve.

To study the kinetics of AHL production, we focused on the analysis of 3-oxo-C10-HSL as it was the dominant AHL for this system. Figure 1a shows the quantitative data obtained by UPLC measurements for 3-oxo-C10-HSL over time. The highest concentration of 124 nM was determined at 10 h and was around four times higher for cultures in the baffled flasks compared with cultures grown in the beaker (33 nM). In the baffled flask experiment, there was a second maximum at 2 h (57 nM), which was also determined in the beaker set-up, only much less pronounced (about 5% of the value in baffled flasks). The shape of the curves was similar for the two experimental set-ups, which was verified by repeating the experiment three times.

Using quantitative chemical analysis (Englmann *et al.*, 2007), 3-oxo-decanoyl-homoserine (3-oxo-C10-HS), which is formed from the homoserine lactone due to the opening of the furan-2-on ring, was detected already during the exponential growth phase (Fig. 1b and Supporting Information, Table S1). The measured 3-oxo-C10-HS concentration reached its maximum of 35 nM at 15 h in the beaker (Fig. 1b), which is about 4 h after the respective AHL maximum appeared. Fluctuations of the concentration–time course were determined when *P. putida* IsoF was grown in the baffled flasks, presumably caused by the individually taken samples. In the beaker experiment, where the samples were taken from the same growing culture, no such fluctuations occurred.

Because 3-oxo-C10-HS decreased again after reaching its maximum after 15 h (Fig. 1b), further degradation had to be taken into consideration. One possibility is the dissociation of the amido group (from AHL or HS) forming a keto derivative of carboxylic acid and serine illustrated in Fig. 4. The *m/z* of 193.1199, corresponding to possible 3-oxo-decanoic acid with an *m/z* error of < 0.1 p.p.m., was detected after 9 h. Although FT-ICR-MS is not the best suitable tool for quantification, the peak intensities can be compared if the samples are treated identically. The experimental data showed an increasing tendency of the 3-oxo-decanoic acid peak intensity with time (not shown).

As controls for biotic *and abiotic* degradation of AHLs by *P. putida* IsoF, we used the AHL-negative mutant F117 and *P. putida* strain KT 2440, which is according to the available complete sequence information devoid of an AHL synthase gene and genes involved in specific AHL degradation (lactonase, acylase). For this, a culture of the respective

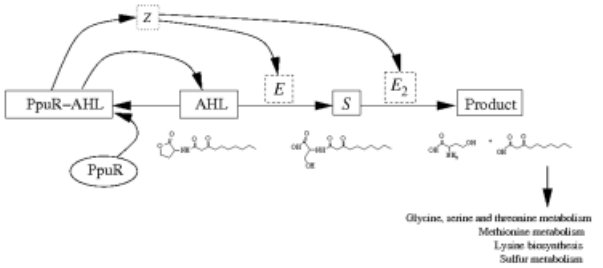

Fig. 4. Regulation pathway. The main players are shown as variables in the model approach in square boxes (AHL; AHL–PpuR complex; *S*, homoserines); the PpuR receptor protein, of which a constant concentration was assumed for the model, is shown in an oval. Biologically well-known components are displayed in solid boxes, hypothetical components in dashed boxes (*E*, putative lactonase; E_2, putative homoserine-degrading enzyme) and the switch variable *z* in a dotted box.

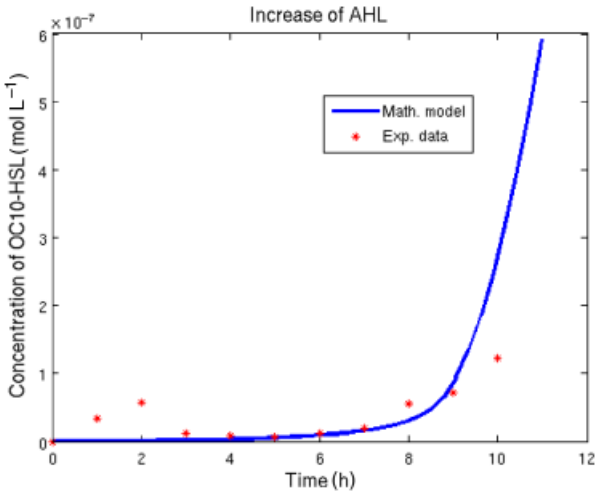

Fig. 5. Fit of the model curve to the experimental data. The data are derived from the kinetic experiment and baffled flasks between hour 0 and 10, which yields values for the model parameters of AHL production (see Table 2). The stars (∗) show the experimental data and the line (-) represents the model.

strain was grown in baffled flasks to an $OD_{436\,nm}$ of 0.2 as this corresponds to the starting point of logarithmic AHL production in strain IsoF. 3-oxo-C10-HSL was added to a final concentration of 100 nM. In the mutant F117, which only bears a knock-out mutation in the AHL synthesis gene, a reduction of the spiked AHL amount by almost 50% could be detected after 3 h and the respective degradation product 3-oxo-C10-HS was found in the supernatant. In contrast, *P. putida* KT2440 did not show any significant formation of homoserine after 3 h, which also demonstrated that abiotic opening of the lactone ring did not occur under the neutral pH conditions of the medium.

AHL production circuit

In order to investigate the basic properties of the nonexpected regulatory pathway of *P. putida* IsoF controlling AHL production, we used standard assumptions for the mathematical model: the AHL–PpuR (a LuxR homologue) complex forms dimers (or even oligomers of length *n*, called the degree of polymerization) (Fuqua & Greenberg, 2002). When these dimers bind to the *lux* box-like element, they induce transcription of for example *ppuI*, which codes for the AHL synthase, leading to a positive feedback loop. A possible feedback on the transcription of *ppuR* was neglected here for the basic model (Goryachev *et al.*, 2006), because it was assumed to be of minor influence. The following simple model for the (net) production of the main AHL (3-oxo-C10-HSL) was used, similar to the approach in (Müller *et al.*, 2006) for a single cell of *V. fischeri*:

$$\dot{A} = -\gamma A + \left(\alpha + \frac{\beta A^n}{A_{\text{thresh}}^n + A^n}\right) \times N(t)$$

It contained a background production of AHL (α), a positive feedback loop leading to an increased production rate of AHL (β), influenced by the actual AHL concentration (A) (especially if exceeding a certain threshold A_{thresh}) and an abiotic degradation term. The population density $N(t)$ followed a logistic growth curve. Mathematical analysis of the stationary states showed a bistable behaviour of this basic model, i.e. a stable 'resting' state and a stable 'activated' state exist, which were partially overlapping (allowing for hysteresis effects).

We used data from the first 10 h of the kinetic experiment with the baffled flasks (see Fig. 1 and Table S1), where the AHL production exceeds the AHL degradation and no further regulation mechanisms, except for the production according to the 'classical' positive feedback loop and the abiotic decay, seemed to play a role. Let A denote the concentration of 3-oxo-C10-HSL. Because there were not enough data points available in the range of activated AHL production, as the AHLs were so rapidly degraded, only the constitutive AHL production rate (α) and the threshold of AHL between constitutive and induced activity could be derived from this experiment (Fig. 5). The abiotic degradation rate (γ) was considered according to the pH-dependent formula in Englmann *et al.* (2007). The other parameter values were determined by a fitting procedure in MATLAB.

In a separate experiment, *P. putida* IsoF cultures (in baffled flasks) were spiked with additional AHL. Because the AHL production was induced faster after this AHL addition than other mechanisms, like additional rapid degradation processes, this procedure allowed an approximation of the increased AHL production rate (β) within 2 h after AHL spiking.

The parameter values, determined using the data of the baffled flasks experiment, are shown in Table 2. Using the

data from the beaker experiment as a control led to values in the same range.

Complete AHL-controlling circuit

Because the temporal accumulation of the AHLs in the medium during the early growth phase of the bacteria under neutral pH conditions showed a rather complex behaviour, the development of a mathematical model was necessary to assess and interpret the time course, essential parts, degradation mode, as well as the production and degradation rates in this system without the need for further experimental set-up. In order to describe the complete pathway controlling AHL production as well as degradation, we addressed the available complexes of PpuR–AHL, or more precisely, their oligomers, and the production rate of AHL depending on these complexes. The degradation was due to an abiotic process, and, additionally, a yet unknown AHL-degrading enzyme. The complete pathway is shown in Fig. 4.

Table 2. Parameter values for AHL production and degradation

Parameter	Name	Value
Constitutive production rate of AHL	α	2.3×10^{-19} mol per cell h^{-1}
Induced production rate of AHL	β	2.3×10^{-18} mol per cell h^{-1}
Degree of polymerization	n	2.5
Threshold of AHL between low and increased activity	A_{thresh}	70 nmol L^{-1}
Abiotic degradation rate of AHL	γ	0.005545 h^{-1}

The values were determined by fitting the basic mathematical model to experimental data from the 36-h kinetic experiment and the spiking experiment.

For the simulations, we used the following model equations (for the meaning of the parameters, see Table 3):

$$\dot{N} = a_1 N\left(1 - \frac{N}{K}\right)$$

$$\dot{A} = -\gamma A + \left(\alpha + \beta \frac{[RA]^m}{[RA_1]^m + [RA]^m}\right) \times N - \kappa_1 E \times A$$

$$[\dot{RA}] = \alpha_1 R \times A - \gamma_1 [RA]$$

$$\dot{z} = -\frac{z}{\tau} + \frac{1}{\tau} \frac{[RA]^m}{[RA_1]^m + [RA]^m}$$

$$\dot{E} = \alpha_2 z \times N - \gamma_2 E$$

When we eliminated the degrading enzyme E (taking α_2 to zero), the model could not explain the AHL dynamics. Even if we adapted the abiotic (and well-validated) degradation rate, the model was not able to reproduce the data (see Fig. 6). Using higher levels of PpuR–AHL complexes in the modelling approach to enable the system to reach AHL levels in the same range as in the basic model in spite of the assumed high abiotic degradation led to an initial bump of AHL that could also be found to some extent in the experiments, but not to a final decrease as observed experimentally (see Fig. 6). Only an enzyme (denoted by E), whose production is regulated by an 'on/off switch' as shown in Fig. 4, could explain the data. The position of the switch (denoted by z, with values between 0, i.e. the 'off state', and 1, the 'on state') was influenced by the present oligomers of PpuR–AHL complexes (denoted by $[RA]$), including some delay for switching to the adequate position. Of course, E was also subject to a degradation process.

The model including the enzyme yields a qualitative behaviour similar to the experimental data (compare Figs 1a, b and 6). To further support this strong hint for the

Table 3. Names of the variables and parameters

Variable	Name	Variable	Name
Bacterial population density	N	Concentration of the AHL-degrading enzyme	E
Concentration of AHL	A	Concentration of HS	S
PpuR–AHL complexes	$[RA]$	Concentration of the HS-degrading enzyme	E_2
Switch variable for enzyme production	z		
Parameter	**Name**	**Parameter**	**Name**
Growth rate of the bacterial population	a_1	Production rate of lactonase	α_2
Capacity of the bacterial population density	K	Degradation rate of lactonase	γ_2
Abiotic degradation rate of AHL	γ	Degradation rate of AHL by lactonase	κ_1
Constitutive production rate of AHL	α	Production rate of the HS-degrading enzyme	α_3
Induced production rate of the AHL	β	Degradation rate of the HS-degrading enzyme	γ_3
Threshold of the PpuRAHL complex between constitutive and induced activity	$[RA_1]$	Degradation rate of HS by the corresponding enzyme	κ_2
Degree of polymerization	m	Delay factor of the switch	τ
Rate of AHL binding to PpuR	α_1	Dissociation rate of the PpuR–AHL complex	γ_1

The list refers to the models describing the regulation system of AHL production/degradation.

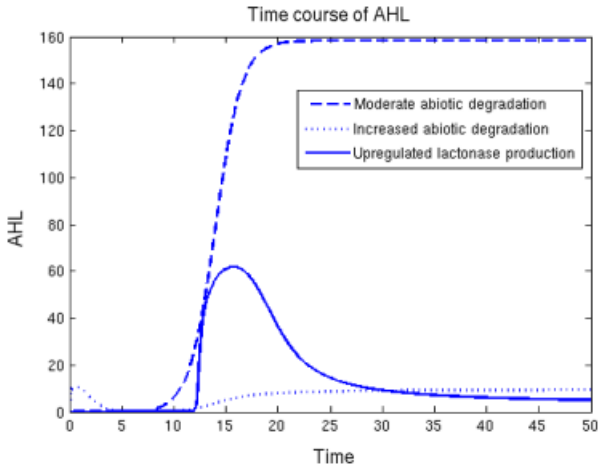

Fig. 6. A model-predicted time course of AHL in three different model versions. The models were calculated with moderate abiotic degradation of AHL, with increased abiotic degradation of AHL and under the assumption of an upregulated lactonase production when exceeding a certain level of AHL–PpuR complexes. Thetime and concentration of AHL are given here in arbitrary units, which are sufficient to check for qualitative behaviour.

existence of such an enzyme, we analysed the possible AHL degradation products in greater detail, in order to examine the nature of this putative enzyme.

Mathematical model of AHL degradation by *P. putida* IsoF

The quantitatively measured homoserine concentrations and the appearance of other AHL-degradation products strongly support the presence of a lactonase and other AHL-degrading enzymes. Interestingly, the homoserines (denoted by S) also do not accumulate, but are degraded (Fig. 1b and Table S1). Their appearance and disappearance can be explained, similar to the AHLs, by the assumption of an additional enzyme, which was produced after the AHLs exceed a certain threshold concentration. The simplest case was considered here, where the production of the homoserine-degrading enzyme (denoted by E_2) is regulated by the same switch like the production of the hypothetic lactonase, resulting in:

$$\dot{S} = \gamma A + \kappa_1 E \times A - \kappa_2 E_2 \times S$$
$$\dot{E}_2 = \alpha_3 z \times N - \gamma_3 E_2$$

Using these equations for qualitative simulations led to the same type of time course for the homoserine concentrations as those found in the experiments (Table S1).

Discussion

Sophisticated metabolite analysis tools (SPE, UPLC, FT-ICR-MS) that allow a quantitative, reliable and sensitive identification of all derivatives and degradation products of AHLs even in trace amounts were applied to analyse the details of the QS-signalling system in *P. putida* IsoF. This enabled us to identify not only the previously described AHLs 3-oxo-C12-HSL, 3-oxo-C10-HSL and 3-oxo-C8-HSL in the supernatant of planktonic *P. putida* IsoF cultures, but a total of 14 different AHLs. They were detected as their sodium adducts and in protonated form with their ^{13}C isotopes, which provides higher reliability of the annotation by FT-ICR-MS. Only 3-oxo-C6-HSL, which was detected in *P. putida* IsoF in previous studies (Steidle *et al.*, 2001), was not identified in the extracted culture supernatant. Either it was not produced under the applied culture conditions or in very low amounts, which due to the high polarity and low mass of 3-oxo-C6-HSL, was not detectable with the applied sample preparation (Li *et al.*, 2006). In accordance with the literature (Steidle *et al.*, 2001), we found oxo-C10-HSL to be the dominant AHL in the cultivation system used. The maximum concentration of 124 nM for this AHL type determined using UPLC is by a factor of almost 10 lower than what was found in other studies (Steidle *et al.*, 2002). However, one has to keep in mind that these published quantitative data stem from a complex medium culture supernatant and the values of around 1 μM given there were only estimated in reference to AHL standard concentrations using thin-layer chromatography (TLC) with bacterial AHL sensor strains. The UPLC analysis performed in our study provides a more accurate and reliable quantification as it is neither dependent on biosensor specificities nor prone to false or biased detection of AHL quantities, for example due to insufficient separation of certain AHL types or influences of AHL-mimicking substances such as diketopiperazines (Holden *et al.*, 1999). This was for example demonstrated by the detection of 3-hydroxy-C10-HSL, which has never been found before in the culture supernatant of *P. putida* IsoF using the standard TLC method. In the literature, this AHL type is also not very commonly mentioned (Shaw *et al.*, 1997; Cha *et al.*, 1998; Bruhn *et al.*, 2005; Khan *et al.*, 2005), but using the combined methods of UPLC and FT-ICR-MS, we were able to prove that it is produced by various other bacterial species such as *Acidovorax* sp. (Fekete *et al.*, 2007) and *Herbaspirillum frisingense* (Rothballer *et al.*, 2008). Probably, it was missed quite frequently in standard AHL-screening procedures due to the lack of suitable sensor strains and the known problem of insufficient separation of oxo- and hydroxy-AHL derivatives of the same chain length with the TLC system (Shaw *et al.*, 1997). Another example for such AHL derivatives, which are obviously only detectable using high-resolution chemical analysis methods, are the whole group of AHLs with double bonds in the side chain. We found three different types (C10:1-HSL, C12:1-HSL and 3-oxo-C12:1-HSL), which are completely new for *P. putida* IsoF. Similar derivatives have been detected only

recently in some strains of marine origin (Wagner-Döbler *et al.*, 2005; Krick *et al.*, 2007). Whether there is a biological role to all these different AHL derivatives can just be speculated, but obviously they all seem to be products of the AHL synthase PpuI as none of the AHLs was detectable in the culture supernatant of the *ppuI* mutant *P. putida* F117.

Although a comparison with AHL quantities published for other bacteria has to be conducted with respect to the method of analysis, culture conditions and time point of sampling, it may be stated that AHL amounts produced by *P. putida* IsoF seem to be on the lower end of the concentration spectrum given in the literature. With bioassays, AHL concentrations in the supernatants of planktonic cultures mostly in the late logarithmic growth phase were determined at 1 μM 3-oxo-C12-HSL for *P. aeruginosa* (Pearson *et al.*, 1995), 16 μM 3-oxo-C8-HSL for *Agrobacterium tumefaciens* (Zhu *et al.*, 1998) and 2 μM 3-oxo-C10-HSL for *Pantoea stewartii* ssp. *stewartii* (Beck von Bodman *et al.*, 1998). GC-MS analysis resulted in values > 600 μM for *P. aeruginosa* biofilms (Charlton *et al.*, 2000), and for a marine *Mesorhizobium* and *Rhizobium* sp., even AHL concentrations in the millimolar range were measured by LC-MS (Krick *et al.*, 2007; Cataldi *et al.*, 2008). The comparatively low concentrations detected for *P. putida* IsoF may be explained by the rapid enzymatic degradation of the AHLs in the liquid cultures, which results in an accumulation of the autoinducer in the culture supernatant. The concentration of all detected AHLs reached its maximum during the early logarithmic growth phase at 10 h in the baffled flasks and at 11 h in the beaker. From this time point, the AHL quantity decreased rapidly down to almost zero after 36 h. Because of the better growth conditions in the baffled flasks, presumably resulting mainly from optimal availability of dissolved oxygen, the cell counts and accordingly also the measured AHL concentration were higher compared with the beaker experiment, but the courses of the graphs derived from the baffled flasks and beaker experiment were almost identical and so were the AHL production rates derived.

When considering the AHL concentrations during the first hours of the kinetic experiment, a first (smaller) temporal increase is measured in the baffled flasks and, to a much lower extent, also in the beaker experiment. A possible explanation for this behaviour is a delay effect: from the preculture, there may still be an increased level of remaining PpuR–AHL complexes present in the cells when the bacteria are shifted to the new environment (beaker or baffled flasks). Thus, AHL can be produced at a higher level at the beginning of the actual experiment, leading to the initial 'jump' in the AHL concentration in the first hours of the experiment. Because the AHLs transferred with the cells from the preculture are diluted 1000-fold in the fresh culture medium, the extracellular AHL concentration in the medium is expected to be initially very low, the same applies for the putative enzymatic degradation. Therefore, an initial high production could not be maintained because PpuR–AHL complexes are disappearing faster than they are formed, until the bacterial population size allows a sufficient accumulation of AHL in the medium, leading to the classical 'jump'. Using appropriate initial conditions for the model equations, we were able to show similar effects of transferring the bacteria from the preculture to the baffled flasks and the beaker. Probably, further effects from the transfer may influence the behaviour, which are not yet known in detail.

The detection and time course of the measured homoserines, as well as the control experiments with *P. putida* F117 and KT2440, led to the conclusion that there is a lactonase activity present in *P. putida* IsoF unaffected by the knock-out of the AHL synthesis gene in strain F117 and not detectable in strain KT2440. As almost 100% of the spiked AHL was rapidly transferred to homoserine, which can only be explained by a lactonase activity, other enzymatic activities, for example by an acylase, do not seem to play a major role in AHL degradation in this system. However, an acylase activity might be responsible for the further degradation of homoserines to fatty acids and, of course, it cannot be ruled out that acylases degrade a minor amount of AHL directly.

A PCR with primer sets designed according to the published sequence data of three lactonase genes (*attM* of *A. tumefaciens*, *aiiA* of *Bacillus* sp. 240B1 and *halS* of *P. aeruginosa*, data not shown) did not result in the amplification of the respective DNA fragment. This could mean that the lactonase gene of *P. putida* IsoF is considerably different from the organisms mentioned and therefore cannot be amplified with primers based on known lactonase gene sequences. The fact that no lactonase gene has been identified in *P. putida* until now, although several laboratories have studied AHL production in this strain, also supports this conclusion. As we found a similar degradation of all AHLs produced by *P. putida* IsoF under the applied cultivation conditions, this might account for the activity of several lactonase enzymes with identical regulation, but different specificity, or one lactonase with a rather large degradation spectrum, such as QsdA described in Uroz *et al.* (2008). However, using the specific primers published in that paper and *P. putida* IsoF genomic DNA as a template for PCR, it was not possible to amplify a DNA fragment with significant similarity to *qsdA*. Finally, we sequenced the whole genome of *P. putida* IsoF with a 454 GS FLX Titanium Pyrosequencer (Roche), which yielded 189 contigs representing a genome size of 5.8 Mb with a 12-fold coverage (data not shown). We then checked for sequence similarities to known AHL lactonase genes using BLAST and performed a quick annotation with the help of the REAL TIME METAGENOMICS software tool (http://bioseed.mcs.anl.gov/~redwards/FIG/RTMg.cgi). We still could not find any similarities to known AHL lactonase genes, but other closely related enzymes such

as metallo-β-lactamases, phosphodiesterases, glucono- and phosphogluconolactonases could be identified. Other members of these enzyme families often exhibit a certain promiscuity regarding their substrate (Mandrich & Manco, 2009) and were also shown to cleave homoserine lactones (Afriat *et al.*, 2006). Such an unspecific lactonase activity could account for the degradation of all AHLs in a system, as it was observed in our study, and might therefore play an equally important role in quorum quenching as the more specific AHL lactonases known to date.

In the modelling approach, which included only the most essential players in order to keep the model as simple as possible, we introduced a switch mechanism, representing an up- or a downregulation of transcription and thus leading to the lactonase production. This switch allows the bacterium to alter its behaviour depending on the actual AHL–PpuR concentration, thus similar to the regulation of the *ppuI* transcription, but including some delay as was found for the homoserine kinetics in the growth experiments and the degradation activity in the spiking experiment. A continuous production of an AHL- and HS-degrading enzyme without any switch did not explain the fast disappearance of AHL; the same applied for an abiotic degradation process. When the repression of PpuI, respectively, AHL production, by RsaL as described for example by Bertani & Venturi (2004) was included in the simulations, slight modulations were obtained in the time course of AHL production, but the fast disappearance of AHL cannot be explained by this mechanism (data not shown). The purpose of RsaL was proposed to be related to maintaining homoeostasis of an elevated AHL concentration or to an on/off switch dramatically increasing or decreasing the AHL production rates (Rampioni *et al.*, 2006). At least under the chosen experimental conditions, both do not seem to occur in *P. putida* IsoF. Thus, the possible benefits of this fine-tuning of the AHL-mediated gene regulation, for example integration of further environmental information, need further investigation.

A novel issue was to determine the AHL production rates on the basis of detailed, time-resolved quantitative data, because most of the publications before did not measure AHL kinetics quantitatively or they only measured secondary effects such as the time course of luminescence, which may differ, for example due to accumulation effects (Kaplan & Greenberg, 1985; Gray & Greenberg, 1992; Lupp *et al.*, 2003). Because the fast disappearance of AHL started to play a role immediately after the beginning of the increased AHL production, we had to adopt two different approaches for the determination of the model parameters describing the pure AHL production (i.e. low production rate, increased production rate, threshold of AHL between low and increased activity, degree of polymerization). The results from the long-time kinetic experiments allowed the assignment of values for all the mentioned parameters by a fitting procedure, except for the increased production rate. From the spiking experiment, we could observe that it took a few hours to initialize the hypothetical lactonase production, i.e. in the first hours, it allowed a good estimation of the increased AHL-production rate. Compared with other tested bacterial species, for example *Burkholderia cepacia* in the activated state, the AHL production rates found for *P. putida* IsoF were in the same range (data not shown). In our example, the production rate increased by one order of magnitude when exceeding the threshold, which was rather weak. For other species, increases of production rates between factors of 10 and 10 000 were reported (Kaplan & Greenberg, 1985; Steidle *et al.*, 2002), and so the parameter value here fits within that range. Thus, the autoinducer-sensing mechanism of *P. putida* includes a positive feedback (leading to a coordination of the bacterial cells), even though it is not very strong under the given conditions. The threshold value of 70 nmol L^{-1} is located in the range of threshold concentrations, as reported previously in the literature (Kaplan & Greenberg, 1985; Gray & Greenberg, 1992).

During the last few years, it became obvious that the autoinducer system itself is tightly regulated depending on environmental and metabolic conditions, i.e. it can be switched off if the conditions do not favour a phenotype decision based on autoinducers (Schuster & Greenberg, 2006). It was ascribed to changing environmental or metabolic conditions, often a transition to the stationary phase and/or starvation, where a cell density-dependent decision of for example exoenzyme production was assumed to be no longer beneficial, and the remaining autoinducer molecules may be used as nutrients (Yates *et al.*, 2002; Zhang *et al.*, 2002; Newton & Fray, 2004; Gonzalez & Keshavan, 2006).

Our results suggest that in *P. putida* IsoF, the inactivation of the autoinducer-signalling system may be regulated by the system itself. Degradation of 3-oxo-C10-HSL in planktonic *P. putida* IsoF cultures started already during the early logarithmic growth phase; thus, starvation or phase transition does not seem to play a role. Instead, the model results indicate that degradation may be linked to the induction by the AHL, with a delay compared with the induction of the increased AHL production. It is not clear whether the start of AHL degradation is caused by an increased production of lactonase or by an activation of an already existent enzyme protein. Although not yet finally proven, the indication that not only AHL production but also degradation seems to be autoregulated leads to the question as to why the cell does not simply stop the production, but additionally actively degrades the autoinducer. In principle, this strategy could allow a higher reactivity of the system, as accumulated signalling molecules representing the past are removed, which subsequently would allow a sensing of the actual

environment by a kind of system-reset (Wang & Leadbetter, 2005; Wang *et al.*, 2007). However, in the case of a continuously high cell density or diffusion limitation, this would result in a new induction, containing no new information. Although such an oscillating sensing system could have advantages concerning efficiency and precision and was suggested to exist in the yeast *Saccharomyces cerevisiae* (Garcia-Ojalvo *et al.*, 2004), there are no hints to its existence in bacteria yet.

There are indications, for example from an evolutionary point of view that QS may primarily work in (attached) microcolonies with fixed cell localization (Diggle *et al.*, 2007; Hense *et al.*, 2007). Furthermore, the most important lifestyle of bacteria seems to be in mixed biofilms formed on all kinds of abiotic and biotic surfaces. Microcolonies as well as biofilms are regularly attached and interact with other organisms, such as plant roots (Schuhegger *et al.*, 2006), zoospores of the macroalga *Ulva* (Tait *et al.*, 2009) or fungi (Hogan *et al.*, 2004). The AHL production of these bacterial assemblages has been shown to influence the behaviour of the colonized organisms considerably, which is termed cross-kingdom signalling. It would be especially advantageous for a root-associated biocontrol bacterium, such as *P. putida* IsoF, if the AHL-signalling system not only consists of a tightly regulated synthesis but also an efficiently regulated degradation and inactivation route. This would avoid the unnecessary accumulation of AHL-signalling compounds, which could also have negative effects, because the plant may start to activate systemic pathogen-resistance responses (Schuhegger *et al.*, 2006), which would challenge the bacterium.

In summary, our results indicate that autoinducer-degrading enzymes may not only be relevant for the degradation and consumption of autoinducers, but may be an integrated, efficiency-optimizing part of QS systems, which enables the bacteria to reset the signal concentration, and thus can adapt rapidly to environmental changes. This systemic level of understanding bacterial communication could only be achieved by a combination of microbiology, analytical chemistry and mathematical modelling.

Acknowledgements

Special thanks are due to Brigitte Look for her help with the extraction. We also greatly appreciate the support of Dr Michael Schmid, including helpful discussions and experimental assistance.

Authors' contribution

A.F., C.K. and M.R. contributed equally to this study.

References

Afriat L, Roodveldt C, Manco G & Tawfik DS (2006) The latent promiscuity of newly identified microbial lactonases is linked to a recently diverged phosphotriesterase. *Biochemistry* **45**: 13677–13686.

Beck von Bodman S, Majerczak DR & Coplin DL (1998) A negative regulator mediates quorum-sensing control of exopolysaccharide production in *Pantoea stewartii* subsp. *stewartii*. *P Natl Acad Sci USA* **95**: 7687–7692.

Bertani I & Venturi V (2004) Regulation of the *N*-acyl homoserine lactone-dependent quorum-sensing system in rhizosphere *Pseudomonas putida* WCS358 and cross-talk with the stationary-phase RpoS sigma factor and the global regulator GacA. *Appl Environ Microb* **70**: 5493–5502.

Bruhn JB, Nielsen KF, Hjelm M, Hansen M, Bresciani J, Schulz S & Gram L (2005) Ecology, inhibitory activity, and morphogenesis of a marine antagonistic bacterium belonging to the *Roseobacter* clade. *Appl Environ Microb* **71**: 7263–7270.

Cataldi TRI, Bianco G & Abate S (2008) Profiling of *N*-acyl-homoserine lactones by liquid chromatography coupled with electrospray ionization and a hybrid quadrupole linear ion-trap and Fourier-transform ion-cyclotron-resonance mass spectrometry (LC-ESI-LTQ-FTICR-MS). *J Mass Spectrom* **43**: 82–96.

Cha C, Gao P, Chen YC, Shaw PD & Farrand SK (1998) Production of acyl-homoserine lactone quorum-sensing signals by gram-negative plant-associated bacteria. *Mol Plant Microbe In* **11**: 1119–1129.

Charlton TS, de Nys R, Netting A, Kumar N, Hentzer M, Givskov M & Kjelleberg S (2000) A novel and sensitive method for the quantification of *N*-3-oxoacyl homoserine lactones using gas chromatography-mass spectrometry: application to a model bacterial biofilm. *Environ Microbiol* **2**: 530–541.

Clark JD & Maaløe O (1967) DNA replication and the division cycle in *Escherichia coli*. *J Mol Biol* **23**: 99–112.

Demuth DR & Lamont RJ (2006) *Bacterial Cell-to-Cell Communication*. Cambridge University Press, Cambridge, UK.

Diggle SP, Gardner A, West SA & Griffin AS (2007) Evolutionary theory of bacterial quorum sensing: when is a signal not a signal? *Philos T R Soc B* **362**: 1241–1249.

Dockery JD & Keener JP (2001) A mathematical model for quorum sensing in *Pseudomonas aeruginosa*. *B Math Biol* **63**: 95–116.

Dubern JF, Lugtenberg BJ & Bloemberg GV (2006) The *ppuI-rsaL-ppuR* quorum-sensing system regulates biofilm formation of *Pseudomonas putida* PCL1445 by controlling biosynthesis of the cyclic lipopeptides putisolvins I and II. *J Bacteriol* **188**: 2898–2906.

Englmann M, Fekete A, Kuttler C *et al.* (2007) The hydrolysis of unsubstituted *N*-acylhomoserine lactones to their homoserine metabolites. Analytical approaches using ultra performance liquid chromatography. *J Chromatogr A* **1160**: 184–193.

Fekete A, Frommberger M, Rothballer M *et al.* (2007) Identification of bacterial *N*-acylhomoserine lactones (AHLs) with a combination of ultra-performance liquid

chromatography (UPLC), ultra-high-resolution mass spectrometry, and *in-situ* biosensors. *Anal Bioanal Chem* **387**: 455–467.

Fuqua C & Greenberg EP (2002) Listening in on bacteria: acyl-homoserine lactone signalling. *Nat Rev Mol Cell Bio* **3**: 685–695.

Fuqua WC, Winans SC & Greenberg EP (1994) Quorum sensing in bacteria: the LuxR–LuxI family of cell density-responsive transcriptional regulators. *J Bacteriol* **176**: 269–275.

Garcia-Ojalvo J, Elowitz MB & Strogatz SH (2004) Modeling a synthetic multicellular clock: repressilators coupled by quorum sensing. *P Natl Acad Sci USA* **101**: 10955–10960.

Gonzalez JE & Keshavan ND (2006) Messing with bacterial quorum sensing. *Microbiol Mol Biol R* **20**: 859–875.

Goryachev AB, Toh DJ & Lee T (2006) Systems analysis of a quorum sensing network: design constraints imposed by the functional requirements, network topology and kinetic constants. *Biosystems* **83**: 178–187.

Götz C, Fekete A, Gebefuegi I *et al.* (2007) Uptake, degradation and chiral discrimination of *N*-acyl-D/L-homoserine lactones by barley (*Hordeum vulgare*) and yam bean (*Pachyrhizus erosus*) plants. *Anal Bioanal Chem* **389**: 1447–1457.

Gray KM & Greenberg EP (1992) Physical and functional maps of the luminescence gene cluster in an autoinducer-deficient *Vibrio fischeri* strain isolated from a squid light organ. *J Bacteriol* **174**: 4384–4390.

Hense BA, Kuttler C, Muller J, Rothballer M, Hartmann A & Kreft JU (2007) Does efficiency sensing unify diffusion and quorum sensing? *Nat Rev Microbiol* **5**: 230–239.

Hogan DA, Vik A & Kolter R (2004) A *Pseudomonas aeruginosa* quorum-sensing molecule influences *Candida albicans* morphology. *Mol Microbiol* **54**: 1212–1223.

Holden MT, Ram Chhabra S, de Nys R *et al.* (1999) Quorum-sensing cross talk: isolation and chemical characterization of cyclic dipeptides from *Pseudomonas aeruginosa* and other gram-negative bacteria. *Mol Microbiol* **33**: 1254–1266.

Horswill AR, Stoodley P, Stewart PS & Parsek MR (2007) The effect of the chemical, biological, and physical environment on quorum sensing in structured microbial communities. *Anal Bioanal Chem* **387**: 371–380.

Huang JJ, Han JI, Zhang LH & Leadbetter JR (2003) Utilization of acyl-homoserine lactone quorum signals for growth by a soil pseudomonad and *Pseudomonas aeruginosa* PAO1. *Appl Environ Microb* **69**: 5941–5949.

Kaplan HB & Greenberg EP (1985) Diffusion of autoinducer is involved in regulation of the *Vibrio fischeri* luminescence system. *J Bacteriol* **163**: 1210–1214.

Khan SR, Mavrodi DV, Jog GJ, Suga H, Thomashow LS & Farrand SK (2005) Activation of the phz operon of *Pseudomonas fluorescens* 2-79 requires the LuxR homolog PhzR, *N*-(3-OH-hexanoyl)-L-homoserine lactone produced by the LuxI homolog PhzI, and a *cis*-acting phz box. *J Bacteriol* **187**: 6517–6527.

Krick A, Kehraus S, Eberl L *et al.* (2007) Marine *Mesorhizobium* sp. produces structurally novel long-chain *N*-acyl-L-homoserine lactones. *Appl Environ Microb* **73**: 2344–2406.

Lee HJ, Lequette Y & Greenberg EP (2006) Activity of purified QscR, a *Pseudomonas aeruginosa* orphan quorum-sensing transcription factor. *Mol Microbiol* **59**: 602–609.

Li X, Fekete A, Englmann M *et al.* (2006) Development and application of a method for the analysis of *N*-acylhomoserine lactones by solid-phase extraction and ultra high pressure liquid chromatography. *J Chromatogr A* **1134**: 186–193.

Lupp C, Urbanowski M, Greenberg EP & Ruby EG (2003) The *Vibrio fischeri* quorum-sensing systems ain and lux sequentially induce luminescence gene expression and are important for persistence in the squid host. *Mol Microbiol* **50**: 319–331.

Mandrich L & Manco G (2009) Evolution in the amidohydrolase superfamily: substrate-assisted gain of function in the E183 K mutant of a phosphotriesterase-like metal-carboxylesterase. *Biochemistry* **48**: 5602–5612.

Müller J, Kuttler C, Hense BA, Rothballer M & Hartmann A (2006) Cell–cell communication by quorum sensing and dimension-reduction. *J Math Biol* **53**: 672–702.

Müller J, Kuttler C & Hense BA (2008) Sensitivity of the quorum sensing system is achieved by low pass filtering. *Biosystems* **92**: 76–81.

Nealson KH (1977) Autoinduction of bacterial luciferase. *Arch Microbiol* **112**: 73–79.

Newton JA & Fray RG (2004) Integration of environmental and host-derived signals with quorum sensing during plant–microbe interactions. *Cell Microbiol* **6**: 213–224.

Ortori CA, Atkinson S, Chhabra SR, Camara M, Williams P & Barret DA (2007) Comprehensive profiling of *N*-acylhomoserine lactones produced by *Yersinia pseudotuberculosis* using liquid chromatography coupled with hybrid quadrupole-linear ion trap mass spectrometry. *Anal Bioanal Chem* **387**: 497–511.

Pearson JP, Passador L, Iglewski BH & Greenberg EP (1995) A second *N*-acylhomoserine lactone signal produced by *Pseudomonas aeruginosa*. *P Natl Acad Sci USA* **92**: 1490–1494.

Rampioni G, Bertani I, Zennaro E, Polticelli F, Venturi V & Leoni L (2006) The quorum-sensing negative regulator RsaL of *Pseudomonas aeruginosa* binds to the *lasI* promoter. *J Bacteriol* **188**: 815–819.

Redfield RJ (2002) Is quorum sensing a side effect of diffusion sensing? *Trends Microbiol* **10**: 365–370.

Rothballer M, Eckert B, Schmid M *et al.* (2008) Endophytic root colonization of gramineous plants by *Herbaspirillum frisingense*. *FEMS Microbiol Ecol* **66**: 85–95.

Schuhegger R, Ihring A, Gantner S *et al.* (2006) Induction of systemic resistance in tomato by *N*-acyl-L-homoserine lactone-producing rhizosphere bacteria. *Plant Cell Environ* **29**: 909–918.

Schuster M & Greenberg EP (2006) A network of networks: quorum sensing gene regulation in *Pseudomonas aeruginosa*. *Int J Med Microbiol* **296**: 73–81.

Shaw PD, Ping G, Daly SL, Cha C, Cronan JE Jr, Rinehart KL & Farrand SK (1997) Detecting and characterizing *N*-acyl-homoserine lactone signal molecules by thin-layer chromatography. *P Natl Acad Sci USA* **94**: 6036–6041.

Smits WK, Kuipers OP & Veening J-W (2006) Phenotypic variation in bacteria: the role of feedback regulation. *Nat Rev Microbiol* **4**: 259–271.

Steidle A, Sigl K, Schuhegger R *et al.* (2001) Visualization of *N*-acylhomoserine lactone-mediated cell–cell communication between bacteria colonizing the tomato rhizosphere. *Appl Environ Microb* **67**: 5761–5770.

Steidle A, Allesen-Holm M, Riedel K, Berg G, Givskov M, Molin S & Eberl L (2002) Identification and characterization of an *N*-acylhomoserine lactone-dependent quorum-sensing system in *Pseudomonas putida* strain IsoF. *Appl Environ Microb* **68**: 6371–6382.

Suarez-Moreno ZR, Caballero-Mellado J & Venturi V (2008) The new group of non-pathogenic plant-associated nitrogen-fixing *Burkholderia* spp. shares a conserved quorum-sensing system, which is tightly regulated by the RsaL repressor. *Microbiology* **154**: 2048–2059.

Tait K, Williamson H, Atkinson S, Williams P, Camara M & Joint I (2009) Turnover of quorum sensing signal molecules modulates cross-kingdom signalling. *Environ Microbiol* **11**: 1792–1802.

Uroz S, Oger PM, Chapelle E, Adeline MT, Faure D & Dessaux Y (2008) A *Rhodococcus qsdA*-encoded enzyme defines a novel class of large-spectrum quorum-quenching lactonases. *Appl Environ Microb* **74**: 1357–1366.

Wagner-Döbler I, Thiel V, Eberl L *et al.* (2005) Discovery of complex mixtures of novel long-chain quorum sensing signals in free-living and host-associated marine alphaproteobacteria. *Chembiochem* **6**: 2195–2206.

Wang YJ & Leadbetter JR (2005) Rapid acyl-homoserine lactone quorum signal biodegradation in diverse soils. *Appl Environ Microb* **71**: 1291–1299.

Wang YJ, Huang JJ & Leadbetter JR (2007) Acyl-{HSL} signal decay: intrinsic to bacterial cell–cell communication. *Adv Appl Microbiol* **61**: 27–58.

Welch M, Todd DE, Whitehead NA, McGowan SJ, Bycroft BW & Salmond GPC (2000) *N*-acyl homoserine lactone binding to the CarR receptor determines quorum-sensing specificity in *Erwinia*. *Embo J* **19**: 631–641.

Williams P, Winzer K, Chan WC & Camara M (2007) Look who's talking: communication and quorum sensing in the bacterial world. *Philos T R Soc B* **362**: 1119–1134.

Yates EA, Philipp B, Buckley C *et al.* (2002) *N*-acylhomoserine lactones undergo lactonolysis in a pH, -temperature-, and acyl chain length-dependent manner during growth of *Yersinia pseudotuberculosis* and *Pseudomonas aeruginosa*. *Infect Immun* **70**: 5635–5646.

Zhang HB, Wang LH & Zhang LH (2002) Genetic control of quorum-sensing signal turnover in *Agrobacterium tumefaciens*. *P Natl Acad Sci USA* **99**: 4638–4643.

Zhu J, Beaber JW, More MI, Fuqua C, Eberhard A & Winans SC (1998) Analogs of the autoinducer 3-oxooctanoyl-homoserine lactone strongly inhibit activity of the TraR protein of *Agrobacterium tumefaciens*. *J Bacteriol* **180**: 5398–5405.

Supporting Information

Additional Supporting Information may be found in the online version of this article:

Table S1. Overview of the concentrations of 3-oxo-C10-HSL and the corresponding HS measured with UPLC, as well as the respective ODs and cell counts from the beaker and baffled flask experiment.

Please note: Wiley-Blackwell is not responsible for the content or functionality of any supporting materials supplied by the authors. Any queries (other than missing material) should be directed to the corresponding author for the article.